HHS Public Access

Author manuscript

Microvasc Res. Author manuscript; available in PMC 2021 May 01.

Published in final edited form as:

Microvasc Res. 2020 May ; 129: 103954. doi:10.1016/j.mvr.2019.103954.

Degradation of Group V Secretory Phospholipase A_2 in Lung Endothelium is Mediated by Autophagy

Lucille N. Meliton[1], **Xiangdong Zhu**[2], **Mary Brown**[3], **Yulia Epshtein**[1], **Takeshi Kawasaki**[4], **Eleftheria Letsiou**[1], **Steven M. Dudek**[1]

[1]Division of Pulmonary, Critical Care, Sleep and Allergy, University of Illinois College of Medicine, Chicago, IL

[2]Department of Emergency Medicine, University of Illinois College of Medicine, Chicago, IL

[3]The Indiana Center for Biological Microscopy, Indiana University School of Medicine

[4]Department of Respirology, Chiba University, Chiba, Japan.

Abstract

Group V secretory phospholipase A_2 ($gVPLA_2$) is a potent inflammatory mediator in mammalian tissues that hydrolyzes phospholipids and initiates eicosanoid biosynthesis. Previous work has demonstrated that multiple inflammatory stimuli induce its expression and secretion in several cell types, including the lung endothelium. However, little is known about the mechanism(s) by which $gVPLA_2$ inflammatory signaling is subsequently downregulated. Therefore, in this study we characterized potential clearance mechanisms for $gVPLA_2$ in lung endothelial cells (EC). We observed that exogenous $gVPLA_2$ is taken up rapidly by nutrient-starved human pulmonary artery EC (HPAEC) in vitro, and its cellular expression subsequently is reduced over several hours. In parallel experiments performed in pulmonary vascular EC isolated from mice genetically deficient in $gVPLA_2$, the degradation of exogenously applied $gVPLA_2$ occurs in a qualitatively similar fashion. This degradation is significantly attenuated in EC treated with ammonium chloride or chloroquine, which are lysosomal inhibitors that block autophagic flux. In contrast, the proteasomal inhibitor MG132 fails to prevent the clearance of $gVPLA_2$. Both immunofluorescence microscopy and proximity ligation assay demonstrate the co-localization of LC3 and $gVPLA_2$ during this process, indicating the association of $gVPLA_2$ with autophagosomes. Nutrient starvation, a known inducer of autophagy, is sufficient to stimulate $gVPLA_2$ degradation. These results suggest that a lysosome-mediated autophagy pathway contributes to $gVPLA_2$ clearance from lung EC. These novel observations advance our understanding of the mechanism by which this key inflammatory enzyme is downregulated in the lung vasculature.

To whom correspondence should be addressed: Steven M. Dudek, M.D., Professor of Medicine, Division of Pulmonary, Critical Care, Sleep, and Allergy, Department of Medicine, University of Illinois at Chicago, CSB 915, 840 S. Wood St., Chicago, IL 60612, sdudek@uic.edu.

Declarations of interest: none

Keywords

Endothelium; autophagy; lysosomes; group V secretory phospholipase A_2; protein degradation

Introduction

Secretory phospholipase A_2 (sPLA$_2$) is a family of lipolytic enzymes that catalyze the cleavage of fatty acids from the *sn*-2 position of phospholipids, leading to the generation of free fatty acids and lysophospholipids (1, 2). The gVPLA$_2$ member of this family is a 14-kDa enzyme with proinflammatory activity that produces several biological effects including airway inflammation, airway hyperresponsiveness, cell adhesion, transcellular communication, and generation of lipid mediators (3–5). In the activated state, intracellular gVPLA$_2$ translocates from the submembrane compartment to the outer cell membrane or nuclear membrane and cleaves membrane phosphatidylcholine resulting in the generation of fatty acids and arachidonic acid metabolites (4–7). An expanding body of work implicates the activation of this enzyme in the pathophysiology of acute lung injury syndromes such as ARDS (acute respiratory distress syndrome) (8). Its activity increases pulmonary endothelial cell (EC) permeability through direct hydrolysis of the cell membrane, and it has a functional role in the inflammatory responses associated with LPS- or ventilator-induced lung injury (4, 9, 10). Thus, a detailed understanding of how the activation and expression of gVPLA$_2$ are regulated in lung tissue may provide important insights into the pathophysiology of inflammatory lung injury. Previously, Kim et al reported that exogenous gVPLA$_2$ added to neutrophils was internalized within 20 minutes and then degraded 45 minutes after addition (3). However, the mechanism that regulates this critical process of gVPLA$_2$ inactivation and clearance has not yet been defined; nor has gVPLA$_2$ degradation been explored in other target cell types such as lung EC.

To maintain cellular homeostasis, protein expression is regulated by the tightly balanced processes of synthesis and degradation. Eukaryotic cells have several fundamental pathways that are involved in protein degradation: the ubiquitin-proteasome, the endo-/lysosomal (endocytosis), and the phago-/lysosomal (autophagy) proteolysis pathways (11). For example, recent work has identified the ubiquitin-proteasome pathway as a key mediator of acute lung injury syndromes (12). Autophagy is an alternative process by which cells autodigest specific portions of their cytoplasmic contents (13, 14). This process is essential for optimal cell function and can play important roles in the development of disease (15, 16). In this study, we sought to characterize the mechanism by which gVPLA$_2$ is degraded in lung EC and identified an important role for autophagy in this process.

Materials and Methods

Reagents

Recombinant human gVPLA$_2$ protein and monoclonal antibody were purchased from Cayman Chemical (Ann Arbor, Mich.) Chloroquine and ammonium chloride were purchased from Sigma (St. Louis, MO). LC3B and SQSTM1/p62 antibodies were acquired from Cell Signaling (Danvers, MA). Immunofluorescent reagents Alexa Fluor 546 and 488

were obtained from Molecular Probes (Grand Island, NY). Duolink Detection Kit was purchased from Olink Bioscience (Uppsala, Sweden).

Human Lung Endothelial Cell Culture

Human pulmonary artery endothelial cells (HPAEC) were obtained from Lonza (Walkersville, MD) and cultured according to the manufacturer's instructions as previously described (9). EC (Passages 6–9) were grown in Endothelial Growth Medium-2 (EGM-2, Lonza), supplemented with 10% fetal bovine serum (FBS; Sigma-Aldrich), at 37°C in a 5% CO_2 incubator.

Isolation and Culture of Mouse Pulmonary Vascular Endothelial Cells (mPVECs)

All experiments involving mice were approved by the Office of Animal Care and Institutional Biosafety for the University of Illinois at Chicago. Pulmonary vascular EC were isolated in a modified approach (17) from previously described mice that are genetically deficient in the *PLA2G5* gene that encodes for $gVPLA_2$ (18) and wild-type mice (C57BL/6). For each isolation, 2–3 mice (6–8 weeks old) were used. The mice were anesthetized with ketamine/xylazine prior to exposure of the lungs by thoracotomy. The lungs were perfused with 30 ml PBS containing 10 U/ml heparin via the right cardiac ventricle and then excised and placed in a 60-mm dish containing DMEM, Collagenase (Worthington Biochemical, New Jersey), Dispase and DNase (Sigma-Aldrich). The tissues were minced under sterile conditions with scissors then strained through a 70 μm cell strainer (BD Bioscience, Germany). Cells were washed and then incubated with the following antibodies: anti-mouse CD16/32, anti-mouse CD31-PECy7, anti-mouse CD45-Alexa 700 (Biolegend, San Diego, California) for 15 minutes at 4°C. Cells were washed and FACS was performed using MoFlo Astrios Cell Sorter (Beckman-Coulter Diagnostics). Endothelial cells were isolated by CD31+/CD45− sorting and then seeded 1.0×10^6 cells/well on gelatin coated 6-well plates and grown in EGM-2 at 37°C in a 5% CO_2 incubator.

Cell treatment

Starvation—Cells (human and mouse EC) were grown to confluence, and then the medium was replaced with basal medium (without FBS) 2 hours prior to the addition of recombinant $gVPLA_2$. Cells were incubated for various times as specified in each experimental set. For one comparison set of experiments, HPAEC were treated with recombinant $gVPLA_2$ in complete media (media containing 10% FBS).

Treatment with Proteasomal and Lysosomal Inhibitors—Cells were grown to confluence, and then the culture growth medium was replaced with basal medium without FBS and containing 10 μM MG132, 10–100 μM chloroquine, or 10 mM ammonium chloride. After 30 minutes, 100 nM recombinant $gVPLA_2$ was added to the medium and incubated for various times as specified in individual experiments.

Immunoblotting analysis—Treated EC were subsequently washed with cold Ca^{2+}/Mg^{2+}-free PBS and lysed with 0.3% SDS buffer containing protease and phosphatase inhibitors (1 mM EDTA, 1 mM PMSF, 1 mM sodium orthovanadate, 1mM sodium fluoride, 0.2 TIU/ml aprotinin, 10 μM leupeptin, 5 μM pepstatin A). Sample proteins were separated

with 15% SDS-PAGE gels and transferred onto nitrocellulose membranes (Bio-Rad). Membranes were then immunoblotted with primary antibodies (1:500–1000, 4°C, overnight) followed by secondary antibodies conjugated to HRP (1:5000, room temperature, 1 hour). Protein expression was detected with enhanced chemiluminescence (Pierce ECL or SuperSignal West Dura, Pierce Biotechnology, Rockford, Ill.) on Biomax MR film (Kodak, Rochester, NY). Multiple blots were scanned and quantitatively analyzed using ImageJ software (National Institutes of Health, Bethesda, Maryland, USA).

Immunofluorescence—EC were grown on gelatinized cover slips before exposure to various conditions as described for individual experiments. EC were then fixed in 3.7% formaldehyde for 10 minutes, permeabilized with 0.25% Triton-X100 for five minutes, washed in PBS, blocked with 2% BSA in TBS-T for one hour, and then incubated for one hour at room temperature with the primary antibody of interest. After washing, EC were incubated with the appropriate secondary antibody conjugated to immunofluorescent dyes for 1 hour at room temperature. Final washing was performed with TBS-T, and coverslips were mounted using Prolong Anti-Fade Reagent (Invitrogen) and analyzed using a Nikon Eclipse TE2000-s inverted microscope and Adobe Photoshop 7.0.

Proximity Ligation Assay for Quantification of Co-localization—Proximity ligation was performed according to the manufacturer's protocol using the Duolink Detection Kit with PLA PLUS and MINUS Probes for mouse and rabbit (Olink Bioscience, Uppsala, Sweden). In brief, an oligonucleotide-conjugated probe (used as secondary antibody) is directed against primary antibodies raised against $gVPLA_2$ or LC3. HPAEC grown on glass slides were incubated with chloroquine and/or $gVPLA_2$ human recombinant protein and then serum starved for 18 hours. Cells were washed with chilled PBS and fixed with 4% paraformaldehyde for 15 min, blocked, and permeabilized with 0.2% Triton-X100 containing 3% BSA, and incubated overnight with appropriate antibodies. DAPI stain was included in the Duolink Detection Kit, while anti-Phalloidin Alexa488 at 1:5000 (Invitrogen) was added during the detection reaction. Specimens were mounted with Vectashield mounting media (Vector Laboratories, Burlingame, CA) and examined with an epi-fluorescence microscope under a ×60 oil objective. Texas-Red signal was analyzed via BlobFinder Imaging Software, developed and optimized for the analysis of images generated by the *in situ* PLA (Uppsala Science Park, Sweden). Five fields were randomly chosen for analysis and averaged, and four separate samples were examined per condition (approximately 60 cells).

Statistical Analysis

Data are expressed as means (±SEM). Student's *t*-test was used for the comparison of two groups. One-way ANOVA was used for multiple-group comparisons, followed by post-hoc analysis with Dunnett's or Tukey's test. Statistical significance was defined as $P \leq 0.05$.

RESULTS

Time-dependent gVPLA$_2$ degradation in lung EC

When gVPLA$_2$ is secreted into the extracellular space, it acts directly on lung EC to induce permeability (9) and is rapidly internalized by cells (3). In the current study, we first determined the time course of gVPLA$_2$ degradation after being internalized by cultured lung EC. Human recombinant gVPLA$_2$ (100 nM) was added to serum-starved HPAECs and incubated from 30 minutes up to 6 hours. This timeframe was selected to model the exposure to extracellular gVPLA$_2$ that occurs in lung EC during the critical early phase of acute lung injury syndromes (4, 7, 9). Whole cell lysates were then analyzed by immunoblotting to demonstrate gVPLA$_2$ levels in EC over time. A time-dependent decline in gVPLA$_2$ levels was observed, with gVPLA$_2$ expression at 6 hours decreased by almost 70% as compared to 30 minutes (0.68±0.04 vs 2.20±0.04, p=.001) (Fig. 1A). Because human lung EC can synthesize gVPLA$_2$ in response to some inflammatory signals (9), we next isolated pulmonary vascular EC (mPVECs) from mice genetically deficient in gVPLA$_2$ (18) to observe the degradation process of exogenous gVPLA$_2$ without the potential confounder of endogenous EC production. After the addition of human recombinant gVPLA$_2$ (100 nM), mPVECs from gVPLA$_2$ knockout mice demonstrated a slower rate of decline in gVPLA$_2$ expression compared to HPAECs (Fig. 1B), with a 50% decline at 48 hours. Similarly, for wild-type murine EC, gVPLA$_2$ protein degradation occurs after 18 hours with a maximum effect at 48 hours (Fig. 1C). No degradation was observed at time points earlier than 4 hours for mouse EC (data not shown).

Degradation of gVPLA$_2$ is not dependent on the ubiquitin-proteasome pathway

To ascertain whether gVPLA$_2$ degradation in lung EC is mediated by the ubiquitin-proteasomal pathway, which is known to play a role in acute lung injury syndromes (12), serum-starved HPAECs were pretreated with the proteasomal inhibitor MG132 (19) 30 minutes before the addition of gVPLA$_2$. Interestingly, proteasomal inhibition with MG132 not only failed to inhibit the degradation of gVPLA$_2$ over time, but instead it was associated with a trend toward accelerated clearance of gVPLA$_2$ that was significant at the later time point (Fig. 2). In gVPLA$_2$-deficient mPVECs, the effects of proteasome inhibition could not be adequately assessed because MG132 caused extensive apoptosis and cell loss at the relevant 48 hour time point. MG132 is known to induce apoptosis in some EC through a caspase-dependent pathway under some conditions (19). Overall, these MG132 data argue against an important role for the proteasomal pathway in gVPLA$_2$ degradation in lung EC.

Degradation of gVPLA$_2$ in lung EC is dependent on a lysosomal pathway

To determine if the lysosomal/autophagic pathway participates in gVPLA$_2$ clearance in lung EC, serum-starved HPAECs were pretreated with the lysosomal inhibitors ammonium chloride (NH_4Cl) or chloroquine (CQ) 30 minutes prior to adding gVPLA$_2$ recombinant protein. CQ is a classical anti-malarial drug that inhibits lysosomal acidification and blocks autophagosome-lysosome fusion (20–23). Both NH_4Cl and CQ neutralize the lysosomal pH to decrease lysozyme activity, cause autophagosome accumulation, and block lysosomal protein degradation (24, 25). In the presence of NH_4Cl, gVPLA$_2$ levels were significantly increased compared to controls at 6 and 18 hours (Fig. 3A–B). Similarly, in HPAEC

pretreated with CQ, $gVPLA_2$ protein degradation is blocked (Fig. 3C). A similar trend was observed in mPVECs isolated from $gVPLA_2$ knockout and WT mice (Fig. 4A–B).

Both NH_4Cl and CQ block autophagic flux and cause autophagosome accumulation. Because of their effect on inhibiting autophagy, proteins associated with the autophagosomes cannot be degraded. To confirm that NH_4Cl or CQ inhibit autophagic flux in $gVPLA_2$-treated EC, we assessed autophagosome accumulation in HPAEC and murine EC by determining the levels of LC3-II and p62 expression (26, 27). We observed a significant increase in the LC3-II/I ratio, a hallmark of autophagy (28, 29), in HPAEC receiving NH_4Cl or CQ and $gVPLA_2$ compared to control cells (Fig. 5A–B), while $gVPLA_2$ alone did not increase the LC3-II/I ratio in these cells under these conditions. A similar pattern was observed in mPVECs isolated from $gVPLA_2$ knockout and WT mice that were incubated with NH_4Cl or CQ and $gVPLA_2$ (Fig. 5C–D). For the mouse cells, LC3-I signal was too weak, and therefore only LC3-II is depicted. Furthermore, the levels of the essential autophagy protein p62/SQSTM1 were increased after treatment with CQ and NH_4Cl in HPAECs (Fig. 6A) and $gVPLA_2$-deficient and WT mPVECs (Fig. 6B–C). Overall, these results support the hypothesis that lysosomal proteolysis/autophagy participates in the degradation of $gVPLA_2$.

These data indicate that $gVPLA_2$ degradation is blocked when autophagy is inhibited, suggesting that autophagy needs to be triggered for $gVPLA_2$ clearance. Moreover, our data demonstrate that $gVPLA_2$ alone does not have a significant effect on the autophagy markers (LC3-II and p62), suggesting that exogenous $gVPLA_2$ does not activate the autophagy process. To further examine whether the experimental conditions under which $gVPLA_2$ is degraded are associated with autophagy, we investigated whether starvation is sufficient to activate autophagy and initiate $gVPLA_2$ degradation. For these experiments, $gVPLA_2$ was added to HPAEC incubated in complete or basal media (starvation). As depicted in Figure 7A, LC3-II expression is increased in nutrient starvation conditions, while p62 levels are decreased, indicating that autophagy is activated. Moreover, $gVPLA_2$ is degraded only in starved HPAEC, while the levels of $gVPLA_2$ remained stable in the unstarved cells (Fig. 7B). Taken together, our data suggest that starvation induces autophagy and $gVPLA_2$ degradation.

During autophagy, the target protein colocalizes with LC3 prior to lysosomal degradation (14). To determine if $gVPLA_2$ colocalizes with LC3, HPAEC were starved and treated with either CQ alone, $gVPLA_2$ alone, or both CQ and $gVPLA_2$ for 18 hours. Immunofluorescence with anti-$gVPLA_2$ and anti-LC3 antibodies revealed cytoplasmic vesicular structures or “puncta” in cells stained with anti-LC3 that overlay with $gVPLA_2$ in the presence of CQ (Fig. 8). To further confirm that $gVPLA_2$ and LC3 colocalize in lung EC, analysis by proximity ligation assay was then performed. The average signal intensity for each condition was quantified and analyzed via BlobFinder Imaging Software. Five fields per condition were randomly chosen for analysis and averaged (approximately 60 cells) (Fig. 9). This PLA analysis yielded positive signals as discrete fluorescent spots constituting evidence of $gVPLA_2$-LC3 interactions occurring at a maximum distance of 40 nm. These interactions were significantly increased in the presence of CQ.

DISCUSSION

To our knowledge, this is the first study to explore the mechanism by which the potent inflammatory mediator, $gVPLA_2$, is degraded and eliminated from lung endothelial cells. Prior work by our group and others has demonstrated that $gVPLA_2$ expression is increased in lung EC in several models of ARDS in vitro and in vivo, while inhibition of $gVPLA_2$ expression or activity is protective in these models (4, 7, 9, 10). Therefore, it is important to characterize how $gVPLA_2$ expression is downregulated in order to better understand the regulation of this inflammatory enzyme. Previous studies have demonstrated that extracellular $gVPLA_2$ is rapidly internalized and degraded in neutrophils (3), but the pathway involved in $gVPLA_2$ degradation has not been determined. In addition, $gVPLA_2$ degradation has not been characterized in other target cell types such as lung EC. For our current study, we focused on clearance of $gVPLA_2$ from human pulmonary artery EC (HPAEC). However, because human lung EC can synthesize $gVPLA_2$ in response to inflammatory signals (9), we also characterized $gVPLA_2$ degradation in mPVECs isolated from mice genetically deficient in $gVPLA_2$ (18) to observe the degradation process of exogenous $gVPLA_2$ without the potential confounder of endogenous EC production. In general, the observed results were qualitatively similar between HPAECs and mPVECs in our experiments.

Eukaryotic cells have several major pathways available for protein degradation: the ubiquitin-proteasome, the endo-/lysosomal (endocytosis), and the phago-/lysosomal (autophagy) proteolysis pathways (11). Of these, our results implicate the autophagy/lysosomal pathway as a route of $gVPLA_2$ clearance in lung EC. Autophagy involves the formation of a double membrane vesicle, called the autophagosome, from discrete portions of the cytosol. Once completely formed, the cytoplasmic material trapped inside the autophagosome is delivered to a lysosome and fused for degradation. In mammalian cells, multiple proteins are involved in autophagy and its regulation. Among these, the microtubule-associated protein 1 light chain 3 (LC3), a mammalian homologue of the Aut7/Apg8 component of the yeast membrane, is a specific autophagosomal marker (11, 30). LC3 attaches to the autophagosomal membrane, and this attachment persists for most of the lifespan of the autophagosome, including the early stages after fusion with the lysosome. Sequestosome-1(p62) binds LC3 and ubiquitinylated proteins and likely serves as a cargo receptor for autophagic degradation (31).

Our studies support the conclusion that $gVPLA_2$ is degraded through autophagy induction and lysosomal degradation in vascular EC. First, inhibitors of lysosomal, but not proteasomal degradation, significantly increased cellular content of $gVPLA_2$ in HPAEC after the addition of exogenous $gVPLA_2$ (Fig. 2–3). In contrast, proteasomal inhibition did not increase levels of $gVPLA_2$ but instead appeared to increase its degradation. This interesting result is consistent with a previous study which demonstrated that MG132 can induce autophagy (32). Secondly, $gVPLA_2$ is degraded when autophagy is induced by nutrient starvation (Fig. 7), a well-established stimulus for autophagy activation (33). Indeed, starved HPAEC had increased levels of LC3-II and decreased levels of p62 compared to non-starved cells, indicating the successful activation of autophagy. Moreover, both immunofluorescence microscopy and proximity ligation assays (Fig. 8–9) demonstrate the colocalization of LC3

and gVPLA$_2$ in the presence of CQ, which in this context serves to arrest the autophagy process so that these interactions can be better observed. This interpretation is further supported by Rhee et al who reported that internalized gVPLA$_2$ colocalized in HEK293 cells with LAMP-2, a lysosome marker (34).

Previous in vitro studies have demonstrated that other members of the sPLA$_2$ family, sPLA$_2$-IB and sPLA$_2$-X, are internalized and degraded via the lysosomal pathway after binding to the M-type phospholipase A$_2$ receptor (PLA$_2$R) (35, 36). These studies implicate a possible role for this receptor in the clearance of extracellular sPLA$_2$. Moreover, PLA$_2$R$^{-/-}$ mice exhibit higher levels of sPLA$_2$-IB and sPLA$_2$-X in bronchoalveolar lavage fluid after ovalbumin treatment than wild type mice, further supporting an important role for PLA$_2$R in the clearance of sPLA$_2$-IB and X (37, 38). PLA$_2$R has a high affinity for sPLA$_2$-IB, -IIA, -IIE, -IIF, and –X (39, 40), but there is no receptor for gVPLA$_2$ (3, 39). It has been reported that gVPLA$_2$ binds to cell membrane via heparan sulfate proteoglycans (3), is associated with lipid rafts, and internalized in a flotillin-dependent pathway (34). In the current study, we observed a substantial colocalization of gVPLA$_2$ with marker proteins specific for autophagosomal degradation (LC3, Fig. 8–9), supporting the conclusion that gVPLA$_2$ degradation requires autophagy induction. In addition, LC3-II levels, a hallmark of autophagy (28, 29), and p62/SQSTM1 expression, another marker for autophagic flux (31, 41), were increased in HPAEC receiving NH$_4$Cl or CQ and gVPLA$_2$ compared to control cells (Fig. 5–6). Thus, conditions associated with inhibition of gVPLA$_2$ degradation (NH$_4$Cl or CQ) are also associated with autophagy inhibition and subsequent autophagosome accumulation.

An important question raised by these observations is whether the endosomal pathway is involved in gVPLA$_2$ degradation. In general, autophagy degrades cytoplasmic components within lysosomes, while endocytosis mediates lysosomal degradation of extracellular and plasma membrane proteins. However, recent studies have found that several membrane proteins are degraded by autophagy rather than endocytosis, including transient receptor potential vanilloid type 1 (42) and connexin 43 (30, 43). As activated and cell membrane-bound gVPLA$_2$ is internalized in a flotillin-dependent pathway (34), it is possible that gVPLA$_2$ is associated with the endosomal trafficking pathway and is transferred to autophagosomes through the endosomes. However, its degradation would not be completed unless autophagy is activated by starvation or other stimuli. Whether gVPLA$_2$ can also be degraded through an endosomal-lysosomal pathway without the involvement of autophagy remains unclear, and further studies are required to answer these questions.

In conclusion, our data indicate that degradation of extracellular gVPLA$_2$ in human lung EC is mediated by intracellular autophagy and lysosomal degradation. These novel observations improve our understanding of the regulation of gVPLA$_2$ expression and provide important insights into how this key inflammatory enzyme is downregulated in the lung vasculature. This work has potential relevance to the pathophysiology of ARDS and other inflammatory lung syndromes.

ACKNOWLEDGEMENTS

We are grateful to Ms. Lakshmi Natarajan for expert technical assistance. This work was supported by AHA 14GRNT20460186 (SD) and NIH R01 HL133059 (SD).

REFERENCES

1. Dennis EA, Cao J, Hsu YH, Magrioti V, Kokotos G. Phospholipase A2 enzymes: physical structure, biological function, disease implication, chemical inhibition, and therapeutic intervention. Chem Rev 2011; 111: 6130–6185. [PubMed: 21910409]
2. Murakami M, Sato H, Miki Y, Yamamoto K, Taketomi Y. A new era of secreted phospholipase A(2). J Lipid Res 2015; 56: 1248–1261. [PubMed: 25805806]
3. Kim KP, Rafter JD, Bittova L, Han SK, Snitko Y, Munoz NM, Leff AR, Cho W. Mechanism of human group V phospholipase A2 (PLA2)-induced leukotriene biosynthesis in human neutrophils. A potential role of heparan sulfate binding in PLA2 internalization and degradation. J Biol Chem 2001; 276: 11126–11134. [PubMed: 11118430]
4. Meliton AY, Munoz NM, Meliton LN, Birukova AA, Leff AR, Birukov KG. Mechanical induction of group V phospholipase A(2) causes lung inflammation and acute lung injury. Am J Physiol Lung Cell Mol Physiol 2013; 304: L689–700. [PubMed: 23525785]
5. Munoz NM, Kim YJ, Meliton AY, Kim KP, Han SK, Boetticher E, O'Leary E, Myou S, Zhu X, Bonventre JV, Leff AR, Cho W. Human group V phospholipase A2 induces group IVA phospholipase A2-independent cysteinyl leukotriene synthesis in human eosinophils. J Biol Chem 2003; 278: 38813–38820. [PubMed: 12796497]
6. Balboa MA, Shirai Y, Gaietta G, Ellisman MH, Balsinde J, Dennis EA. Localization of group V phospholipase A2 in caveolin-enriched granules in activated P388D1 macrophage-like cells. J Biol Chem 2003; 278: 48059–48065. [PubMed: 12963740]
7. Munoz NM, Meliton AY, Meliton LN, Dudek SM, Leff AR. Secretory group V phospholipase A2 regulates acute lung injury and neutrophilic inflammation caused by LPS in mice. Am J Physiol Lung Cell Mol Physiol 2009; 296: L879–887. [PubMed: 19286925]
8. Kitsiouli E, Nakos G, Lekka ME. Phospholipase A2 subclasses in acute respiratory distress syndrome. Biochim Biophys Acta 2009; 1792: 941–953. [PubMed: 19577642]
9. Dudek SM, Munoz NM, Desai A, Osan CM, Meliton AY, Leff AR. Group V phospholipase A2 mediates barrier disruption of human pulmonary endothelial cells caused by LPS in vitro. Am J Respir Cell Mol Biol 2011; 44: 361–368. [PubMed: 20448053]
10. Munoz NM, Desai A, Meliton LN, Meliton AY, Zhou T, Leff AR, Dudek SM. Group V phospholipase A(2) increases pulmonary endothelial permeability through direct hydrolysis of the cell membrane. Pulm Circ 2012; 2: 182–192. [PubMed: 22837859]
11. Knecht E, Aguado C, Carcel J, Esteban I, Esteve JM, Ghislat G, Moruno JF, Vidal JM, Saez R. Intracellular protein degradation in mammalian cells: recent developments. Cell Mol Life Sci 2009; 66: 2427–2443. [PubMed: 19399586]
12. Magnani ND, Dada LA, Sznajder JI. Ubiquitin-proteasome signaling in lung injury. Transl Res 2018; 198: 29–39. [PubMed: 29752900]
13. Mizushima N Autophagy: process and function. Genes Dev 2007; 21: 2861–2873. [PubMed: 18006683]
14. Yang Z, Klionsky DJ. Eaten alive: a history of macroautophagy. Nat Cell Biol 2010; 12: 814–822. [PubMed: 20811353]
15. Nakahira K, Pabon Porras MA, Choi AM. Autophagy in Pulmonary Diseases. Am J Respir Crit Care Med 2016; 194: 1196–1207. [PubMed: 27579514]
16. Ryter SW, Bhatia D, Choi ME. Autophagy: A Lysosome-Dependent Process with Implications in Cellular Redox Homeostasis and Human Disease. Antioxid Redox Signal 2019; 30: 138–159. [PubMed: 29463101]
17. Kawasaki T, Nishiwaki T, Sekine A, Nishimura R, Suda R, Urushibara T, Suzuki T, Takayanagi S, Terada J, Sakao S, Tatsumi K. Vascular Repair by Tissue-Resident Endothelial Progenitor Cells in

Endotoxin-Induced Lung Injury. Am J Respir Cell Mol Biol 2015; 53: 500–512. [PubMed: 25719275]

18. Satake Y, Diaz BL, Balestrieri B, Lam BK, Kanaoka Y, Grusby MJ, Arm JP. Role of group V phospholipase A2 in zymosan-induced eicosanoid generation and vascular permeability revealed by targeted gene disruption. J Biol Chem 2004; 279: 16488–16494. [PubMed: 14761945]
19. Han YH, Moon HJ, You BR, Yang YM, Kim SZ, Kim SH, Park WH. MG132, a proteasome inhibitor, induced death of calf pulmonary artery endothelial cells via caspase-dependent apoptosis and GSH depletion. Anticancer Res 2010; 30: 879–885. [PubMed: 20393010]
20. Dunmore BJ, Drake KM, Upton PD, Toshner MR, Aldred MA, Morrell NW. The lysosomal inhibitor, chloroquine, increases cell surface BMPR-II levels and restores BMP9 signalling in endothelial cells harbouring BMPR-II mutations. Hum Mol Genet 2013; 22: 3667–3679. [PubMed: 23669347]
21. Schonewolf CA, Mehta M, Schiff D, Wu H, Haffty BG, Karantza V, Jabbour SK. Autophagy inhibition by chloroquine sensitizes HT-29 colorectal cancer cells to concurrent chemoradiation. World J Gastrointest Oncol 2014; 6: 74–82. [PubMed: 24653797]
22. Yoon YH, Cho KS, Hwang JJ, Lee SJ, Choi JA, Koh JY. Induction of lysosomal dilatation, arrested autophagy, and cell death by chloroquine in cultured ARPE-19 cells. Invest Ophthalmol Vis Sci 2010; 51: 6030–6037. [PubMed: 20574031]
23. Mauthe M, Orhon I, Rocchi C, Zhou X, Luhr M, Hijlkema KJ, Coppes RP, Engedal N, Mari M, Reggiori F. Chloroquine inhibits autophagic flux by decreasing autophagosome-lysosome fusion. Autophagy 2018; 14: 1435–1455. [PubMed: 29940786]
24. Myeku N, Figueiredo-Pereira ME. Dynamics of the degradation of ubiquitinated proteins by proteasomes and autophagy: association with sequestosome 1/p62. J Biol Chem 2011; 286: 22426–22440. [PubMed: 21536669]
25. Saetre F, Korseberg Hagen L, Engedal N, Seglen PO. Novel steps in the autophagic-lysosomal pathway. FEBS J 2015.
26. Tanida I, Minematsu-Ikeguchi N, Ueno T, Kominami E. Lysosomal turnover, but not a cellular level, of endogenous LC3 is a marker for autophagy. Autophagy 2005; 1: 84–91. [PubMed: 16874052]
27. Barth S, Glick D, Macleod KF. Autophagy: assays and artifacts. J Pathol 2010; 221: 117–124. [PubMed: 20225337]
28. Mizushima N, Yoshimori T. How to interpret LC3 immunoblotting. Autophagy 2007; 3: 542–545. [PubMed: 17611390]
29. Tasdemir E, Galluzzi L, Maiuri MC, Criollo A, Vitale I, Hangen E, Modjtahedi N, Kroemer G. Methods for assessing autophagy and autophagic cell death. Methods Mol Biol 2008; 445: 29–76. [PubMed: 18425442]
30. Falk MM, Fong JT, Kells RM, O'Laughlin MC, Kowal TJ, Thevenin AF. Degradation of endocytosed gap junctions by autophagosomal and endo-/lysosomal pathways: a perspective. J Membr Biol 2012; 245: 465–476. [PubMed: 22825714]
31. Pankiv S, Clausen TH, Lamark T, Brech A, Bruun JA, Outzen H, Overvatn A, Bjorkoy G, Johansen T. p62/SQSTM1 binds directly to Atg8/LC3 to facilitate degradation of ubiquitinated protein aggregates by autophagy. J Biol Chem 2007; 282: 24131–24145. [PubMed: 17580304]
32. Lan D, Wang W, Zhuang J, Zhao Z. Proteasome inhibitor-induced autophagy in PC12 cells overexpressing A53T mutant alpha-synuclein. Mol Med Rep 2015; 11: 1655–1660. [PubMed: 25434876]
33. Klionsky DJ, et al. Guidelines for the use and interpretation of assays for monitoring autophagy (3rd edition). Autophagy 2016; 12: 1–222. [PubMed: 26799652]
34. Rhee HJ, Ji L, Kim SH, Lee J. Human group V secretory phospholipase A2 is associated with lipid rafts and internalized in a flotillindependent pathway. Int J Mol Med 2013; 32: 1126–1136. [PubMed: 24042857]
35. Zvaritch E, Lambeau G, Lazdunski M. Endocytic properties of the M-type 180-kDa receptor for secretory phospholipases A2. J Biol Chem 1996; 271: 250–257. [PubMed: 8550569]

36. Yokota Y, Notoya M, Higashino K, Ishimoto Y, Nakano K, Arita H, Hanasaki K. Clearance of group X secretory phospholipase A(2) via mouse phospholipase A(2) receptor. FEBS Lett 2001; 509: 250–254. [PubMed: 11741598]

37. Mishina H, Watanabe K, Tamaru S, Watanabe Y, Fujioka D, Takahashi S, Suzuki K, Nakamura T, Obata JE, Kawabata K, Yokota Y, Inoue O, Murakami M, Hanasaki K, Kugiyama K. Lack of phospholipase A2 receptor increases susceptibility to cardiac rupture after myocardial infarction. Circ Res 2014; 114: 493–504. [PubMed: 24305469]

38. Tamaru S, Mishina H, Watanabe Y, Watanabe K, Fujioka D, Takahashi S, Suzuki K, Nakamura T, Obata JE, Kawabata K, Yokota Y, Murakami M, Hanasaki K, Kugiyama K. Deficiency of phospholipase A2 receptor exacerbates ovalbumin-induced lung inflammation. J Immunol 2013; 191: 1021–1028. [PubMed: 23817419]

39. Rouault M, Le Calvez C, Boilard E, Surrel F, Singer A, Ghomashchi F, Bezzine S, Scarzello S, Bollinger J, Gelb MH, Lambeau G. Recombinant production and properties of binding of the full set of mouse secreted phospholipases A2 to the mouse M-type receptor. Biochemistry 2007; 46: 1647–1662. [PubMed: 17279628]

40. Hanasaki K, Arita H. Phospholipase A2 receptor: a regulator of biological functions of secretory phospholipase A2. Prostaglandins Other Lipid Mediat 2002; 68–69: 71–82.

41. Jiang P, Mizushima N. LC3- and p62-based biochemical methods for the analysis of autophagy progression in mammalian cells. Methods 2015; 75: 13–18. [PubMed: 25484342]

42. Ahn S, Park J, An I, Jung SJ, Hwang J. Transient receptor potential cation channel V1 (TRPV1) is degraded by starvation- and glucocorticoid-mediated autophagy. Mol Cells 2014; 37: 257–263. [PubMed: 24658385]

43. Lichtenstein A, Minogue PJ, Beyer EC, Berthoud VM. Autophagy: a pathway that contributes to connexin degradation. J Cell Sci 2011; 124: 910–920. [PubMed: 21378309]

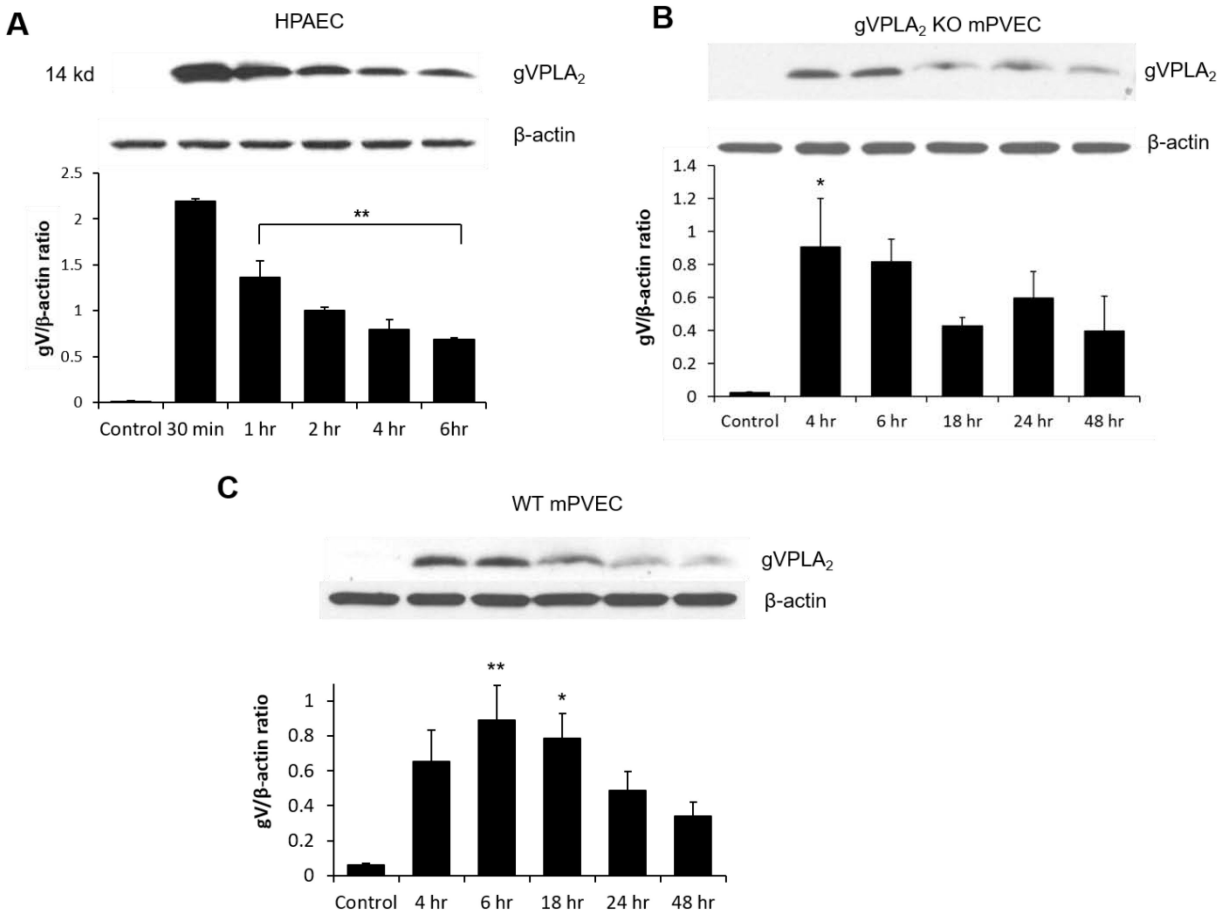

Figure 1. Time-dependent gVPLA$_2$ degradation in human and mouse lung EC.

(A) Serum-starved HPAECs were stimulated with recombinant gVPLA$_2$ protein (100 nM). Cell lysates were then collected at various time points post incubation, and western blot analysis of gVPLA$_2$ expression was performed. N=3 independent experiments. ***P*<0.01 vs. the 30 min time point. Mouse PVECs isolated from (B) gVPLA$_2$ knockout mice or (C) wild-type (WT) mice were serum starved and stimulated with recombinant gVPLA$_2$ protein (100 nM). Cell lysates were then collected at various time points post incubation, and western blot analysis of gVPLA$_2$ expression was performed. N=3–5 independent experiments. *p<0.05, ***p*<0.01 vs. control. Levels of gVPLA$_2$ were normalized to β-actin protein. Representative blots and densitometric quantification are shown.

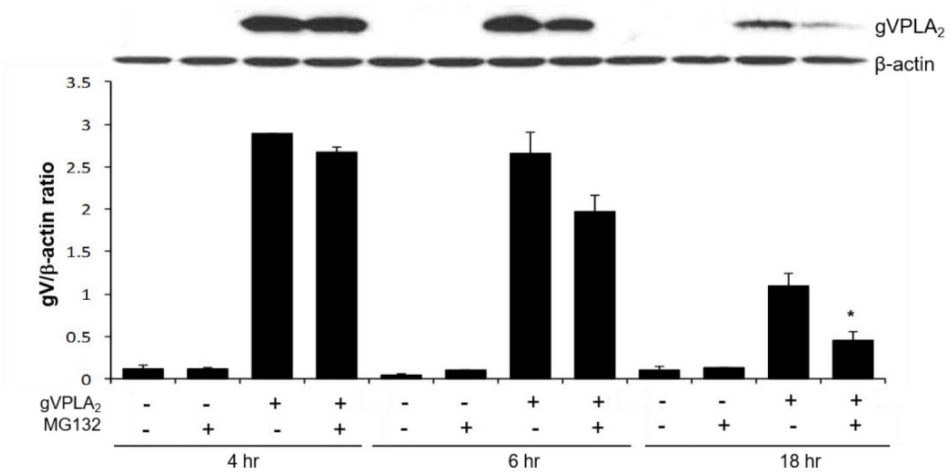

Figure 2. Proteasomal inhibition does not prevent the degradation of gVPLA$_2$.

Serum-starved HPAECs were treated with MG132 (10 μM) for 30 minutes before the addition of 100 nM gVPLA$_2$ recombinant protein. Cell lysates were then collected at 4, 6 and 18-hour time points for western blot analysis of gVPLA$_2$ expression. N=3 independent experiments. *p<0.05 vs. gVPLA$_2$ alone for the indicated time point. Levels of gVPLA$_2$ were normalized to β-actin protein. Representative blots and densitometric quantification are shown.

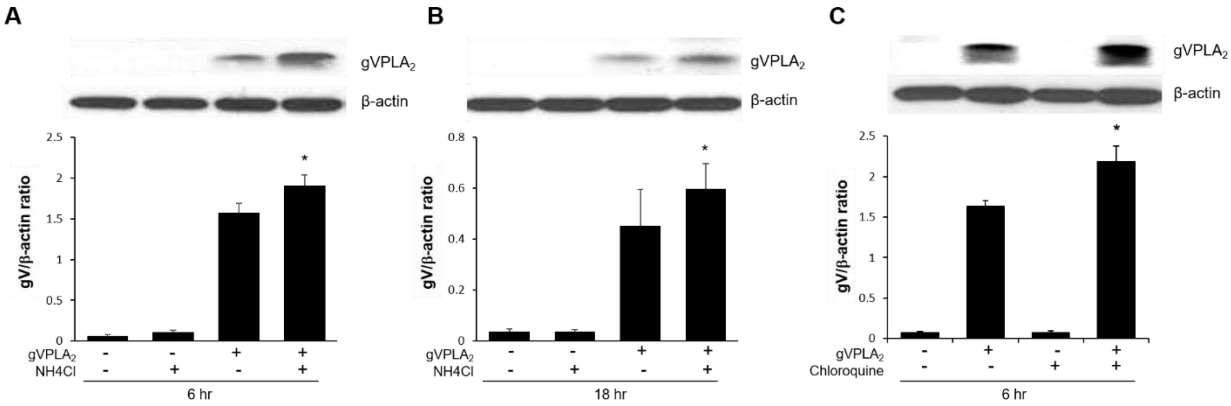

Figure 3. Lysosomal inhibition attenuates the degradation of gVPLA$_2$ in HPAEC.

Serum-starved HPAECs were treated with lysosomal inhibitors, (A-B) 10 mM ammonium chloride (NH_4Cl), or (C) 100 μM chloroquine, 30 minutes prior to adding 100 nM gVPLA$_2$ recombinant protein. Cell lysates were collected at indicated time points for western blot analysis of gVPLA$_2$ expression. N=3–5 independent experiments. Levels of gVPLA$_2$ were normalized to β-actin protein. *$p \leq 0.05$ vs. gVPLA$_2$ alone. Representative blots and densitometric quantification are shown.

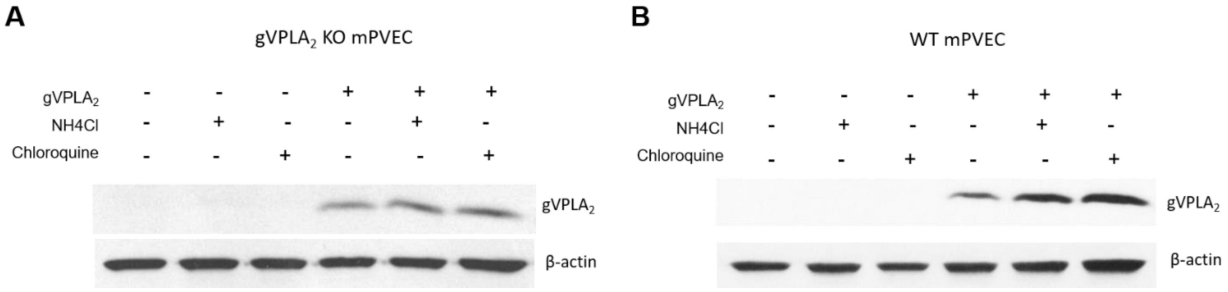

Figure 4. Lysosomal inhibition attenuates the degradation of gVPLA$_2$ in murine lung EC.

Lung ECs were isolated from (A) gVPLA$_2$ KO or (B) wild-type (WT) mice. Serum-starved EC were treated with ammonium chloride (NH_4Cl, 10 mM), or chloroquine (100 μM) 30 minutes prior to addition of 100 nM gVPLA$_2$ recombinant protein. Cell lysates were collected after 48 hours for western blot analysis of gVPLA$_2$ expression. Depicted are representative blots of three independent experiments.

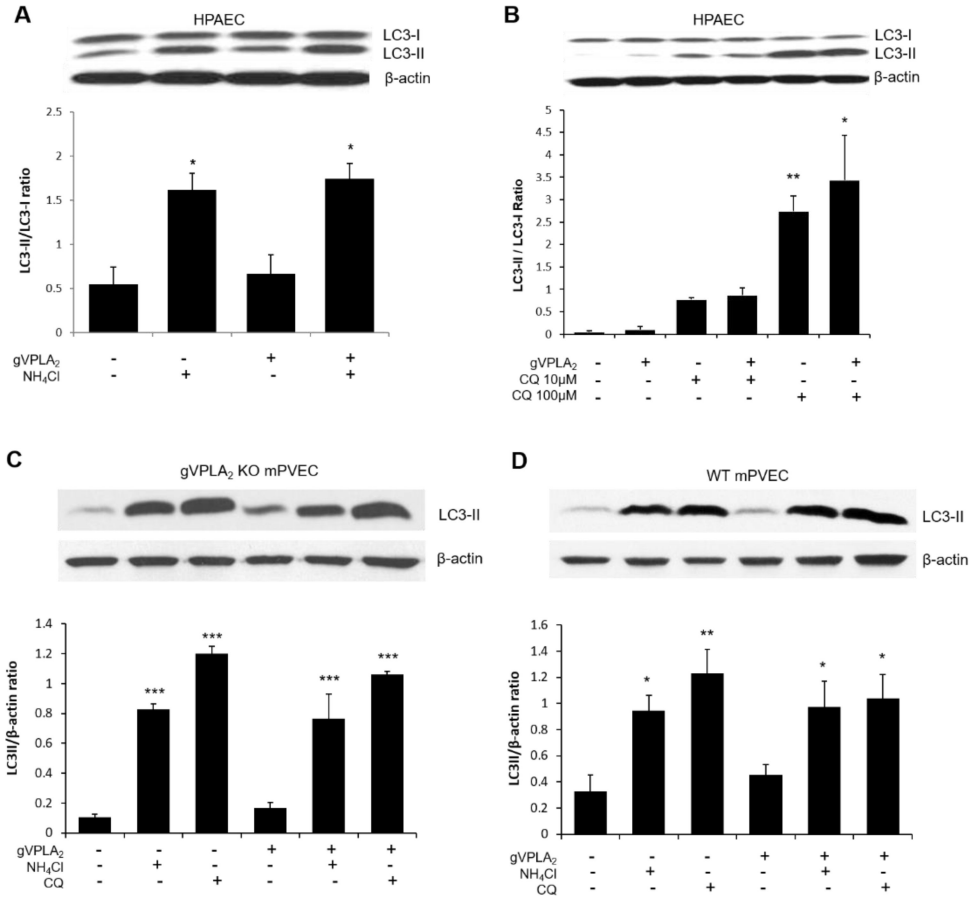

Figure 5. Effects of chloroquine and ammonium chloride on LC3-II expression in $gVPLA_2$-treated lung EC.

Serum-starved HPAECs were pretreated either with (A) 10 mM NH_4Cl or (B) 10–100 μM chloroquine (CQ), for 30 minutes before the addition of 100 nM $gVPLA_2$ recombinant protein. Cell lysates were collected after 6 hours for western blot analysis of LC3-II/LC3-I expression. N=3 independent experiments. * $p<0.05$; ** $p<0.01$ vs. control untreated EC. Mouse PVECs isolated from (C) $gVPLA_2$ knockout or (D) wild-type (WT) mice were pre-treated with 10 mM NH_4Cl or 100 μM CQ for 30 minutes, prior to the addition of 100 nM $gVPLA_2$. Cell lysates were collected after 48 hours for western blot analysis of LC3-II expression. N=3 independent experiments. *$p<0.05$, **p<0.01, ***p<0.001 vs. $gVPLA_2$ alone and vs. control untreated EC. Representative blots and densitometric quantification are shown.

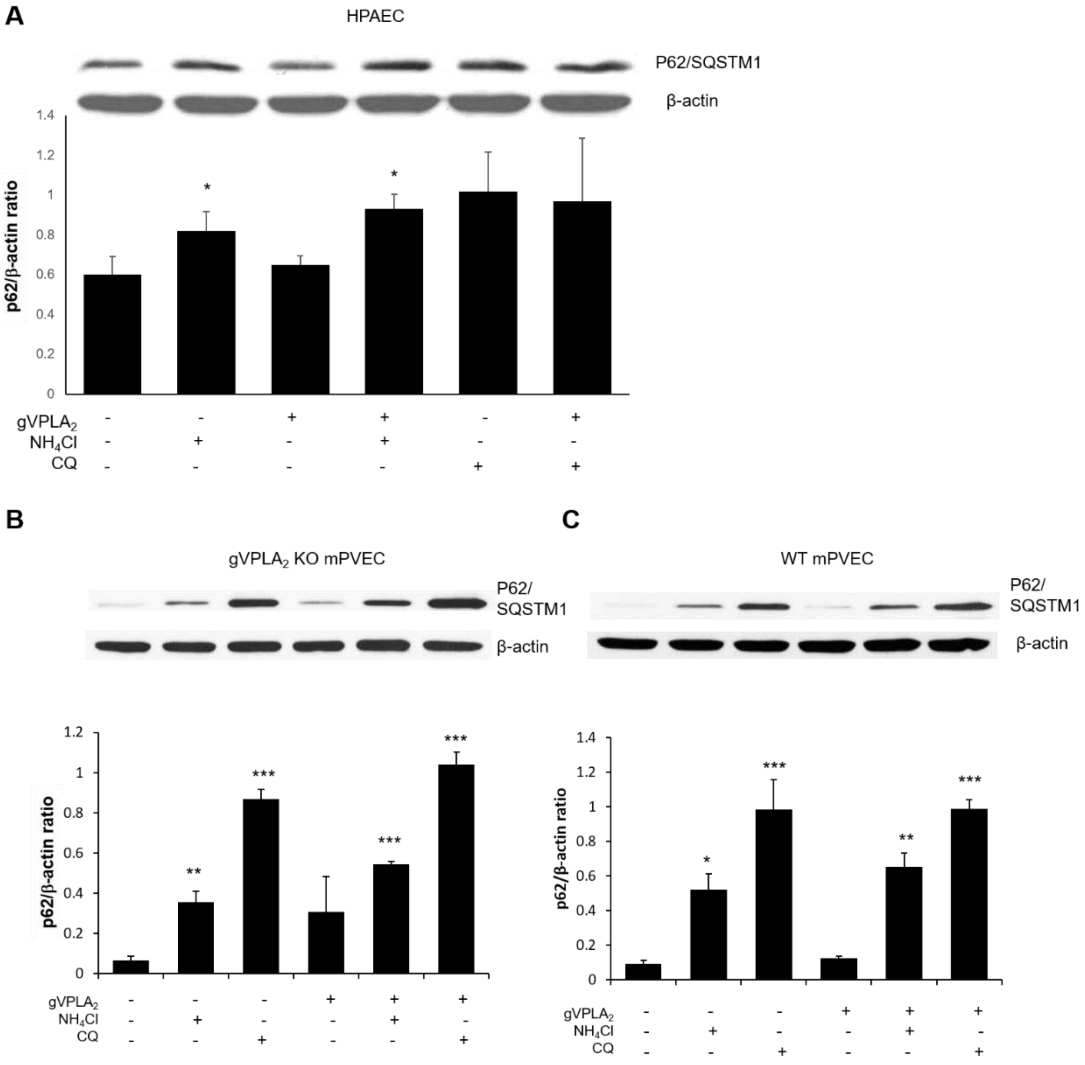

Figure 6. Effects of chloroquine and ammonium chloride on p62/SQSTM1 expression in gVPLA$_2$-treated lung EC.

Serum-starved HPAECs were pretreated either with (A) 10 mM NH_4Cl or (B) 100 μM chloroquine (CQ), for 30 minutes before the addition of 100 nM gVPLA$_2$ recombinant protein. Cell lysates were collected after 6 hours for western blot analysis of p62/SQSTM1 expression. N=5 independent experiments. * p<0.05 vs. control untreated EC. Mouse PVECs isolated from (B) gVPLA$_2$ knockout and (C) wild-type (WT) mice were pre-treated with 10 mM NH_4Cl or 100 μM CQ for 30 minutes, prior to the addition of 100 nM gVPLA$_2$. Cell lysates were collected after 48 hours for western blot analysis of p62/SQSTM1 expression. N=3 independent experiments. *p<0.05, **p<0.01, ***p<0.001 vs. control untreated EC. Representative blots and densitometric quantification are shown.

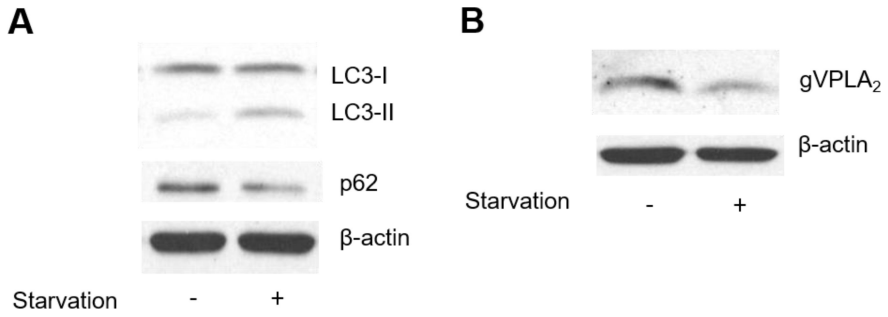

Figure 7. Effect of starvation on gVPLA$_2$ expression.

Recombinant gVPLA$_2$ was added to HPAEC grown in complete media (no starvation) vs basal media (starvation). (A) Cell lysates were collected after 6 hours for western blot analysis of LC3 and p62 expression to assess the autophagy status. (B) gVPLA$_2$ levels were assessed under these serum conditions by western blotting. Representative blots of three independent experiments are shown.

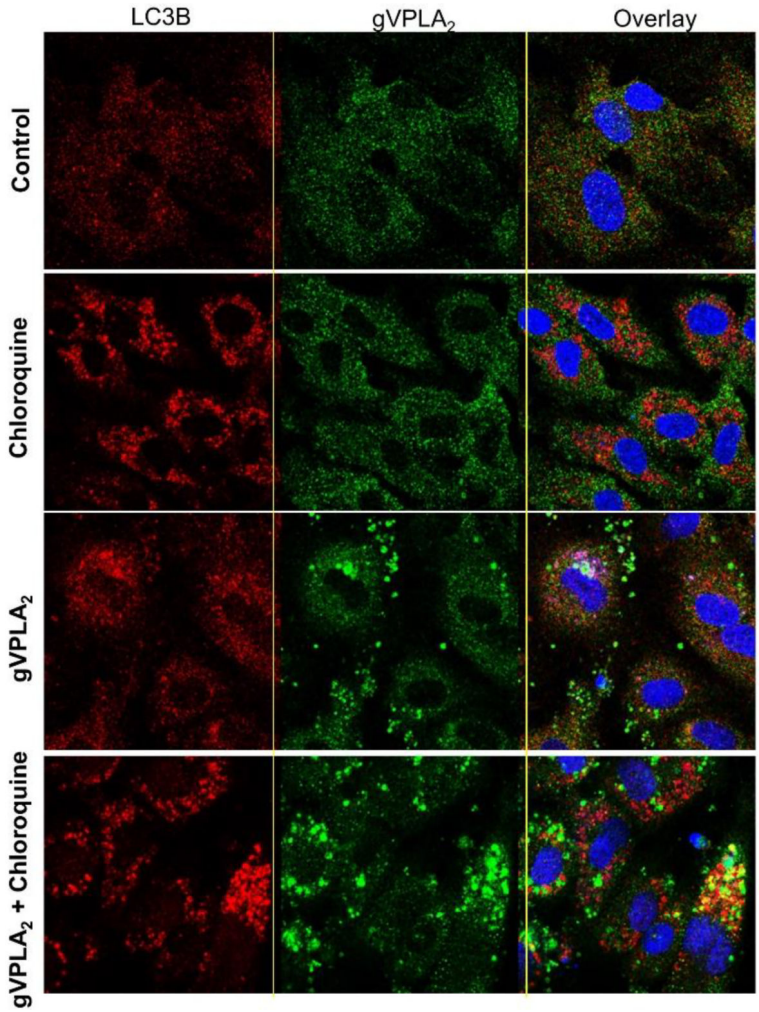

Figure 8. LC3 co-localizes with gVPLA$_2$ in lung EC treated with chloroquine.

Serum-starved HPAECs were incubated for 18 hours with either vehicle control, 100 μM chloroquine alone, 100 nM human recombinant gVPLA$_2$ alone, or both CQ and gVPLA$_2$. The cells were then subjected to immunofluorescence using anti-LC3 (RED) and anti-gVPLA$_2$ (GREEN) antibodies. Nuclei were stained with DAPI (BLUE). Cytoplasmic vesicular structures or "puncta" were observed. Overlay of images demonstrate co-localization (YELLOW) of LC3 and gVPLA$_2$ in the presence of CQ. Images are representative of 4 independent experiments.

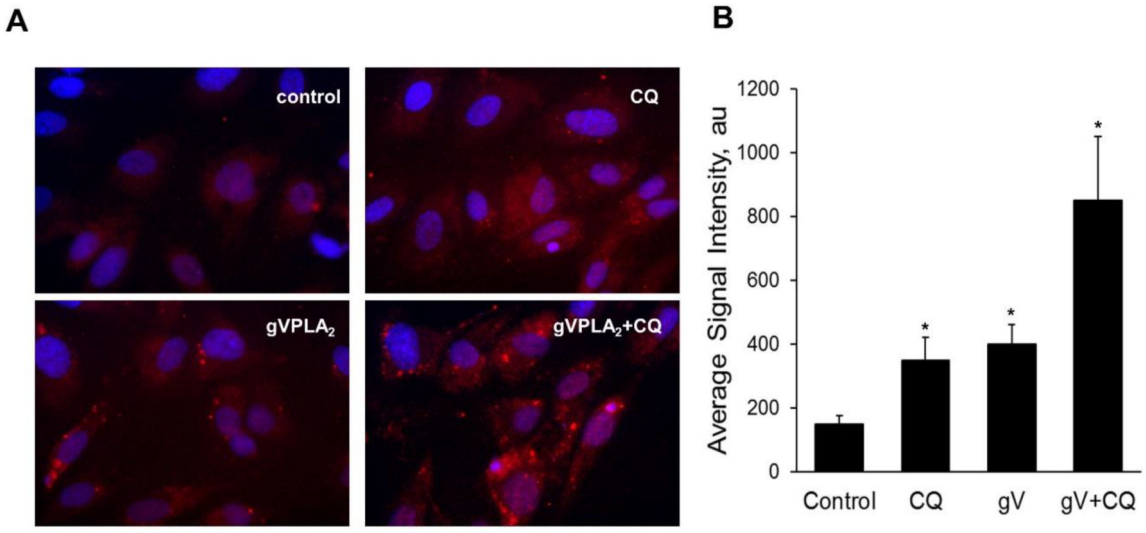

Figure 9. Chloroquine significantly increases LC3-gVPLA$_2$ co-localization in lung ECs.

(A) Serum-starved HPAECs were incubated for 18 hours with either vehicle control, 100 μM chloroquine alone, 100 nM human recombinant gVPLA$_2$ alone, or both CQ and gVPLA$_2$. The close association of gVPLA$_2$ with LC3B was detected by *in situ* proximity ligation assay (*red dots*). Representative images are shown. (B) Average signal intensity for each condition was quantified and analyzed via BlobFinder Imaging Software, developed and optimized for the analysis of images generated by the *in situ* PLA (Uppsala Science Park, Sweden). Five fields per condition were randomly chosen for analysis and averaged (~60 cells). N = 5/condition, * $p < 0.05$ vs. control.